INFECTION AND IMMUNITY, Oct. 2009, p. 4643–4653 Vol. 77, No. 10
0019-9567/09/$08.00+0 doi:10.1128/IAI.01433-08

Antigen Display, T-Cell Activation, and Immune Evasion during Acute and Chronic Ehrlichiosis[▽]

Bisweswar Nandi,[1] Madhumouli Chatterjee,[1] Kathryn Hogle,[1] Maura McLaughlin,[1] Katherine MacNamara,[1] Rachael Racine,[2] and Gary M. Winslow[1,2]*

Wadsworth Center, New York State Department of Health, P.O. Box 22002, Albany, New York 12201-2002,[1] and The Department of Biomedical Sciences, School of Public Health, University at Albany, Albany, New York 12201-0509[2]

Received 21 November 2008/Returned for modification 29 December 2008/Accepted 16 July 2009

How spatial and temporal changes in major histocompatibility complex/peptide antigen presentation to CD4 T cells regulate CD4 T-cell responses during intracellular bacterial infections is relatively unexplored. We have shown that immunization with an ehrlichial outer membrane protein, OMP-19, protects mice against fatal ehrlichial challenge infection, and we identified a CD4 T-cell epitope (IA^b/OMP-$19_{107-122}$) that elicited CD4 T cells following either immunization or infection. Here, we have used an IA^b/OMP-$19_{107-122}$-specific T-cell line to monitor antigen display ex vivo during acute and chronic infection with *Ehrlichia muris*, a bacterium that establishes persistent infection in C57BL/6 mice. The display of IA^b/OMP-$19_{107-122}$ by host antigen-presenting cells was detected by measuring intracellular gamma interferon (IFN-γ) production by the T-cell line. After intravenous infection, antigen presentation was detected in the spleen, peritoneal exudate cells, and lymph nodes, although the kinetics of antigen display differed among the tissues. Antigen presentation and bacterial colonization were closely linked in each anatomical location, and there was a direct relationship between antigen display and CD4 T-cell effector function. Spleen and lymph node dendritic cells (DCs) were efficient presenters of IA^b/OMP-$19_{107-122}$, demonstrating that DCs play an important role in ehrlichial infection and immunity. Chronic infection and antigen presentation occurred within the peritoneal cavity, even in the presence of highly activated CD4 T cells. These data indicated that the ehrlichiae maintain chronic infection not by inhibiting antigen presentation or T-cell activation but, in part, by avoiding signals mediated by activated T cells.

Major histocompatibility complex class II (MHC-II)-restricted CD4 T cells are well known to contribute to immunity during many intracellular bacterial infections. Less is known, however, regarding when and where during infection MHC-II/peptide antigens are available to generate and maintain protective T-cell immunity. Some intracellular bacteria can modulate antigen presentation to CD4 T cells (7, 30, 49), although many intracellular bacteria elicit both acute and chronic CD4 T-cell responses, even in the absence of sterilizing immunity (25, 29, 33, 48, 50). How CD4 T-cell responses are initiated and maintained during both acute and chronic infection is, therefore, an ongoing question that is relevant to a number of bacterial, viral, and parasitic infections. Knowledge of T-cell antigen presentation will aid in understanding how, during acute infections, the quantity and quality of the antigens presented serve to regulate T-cell differentiation and memory development. During chronic infections, persistent antigen display likely regulates effector T-cell populations that are essential for the maintenance of immunity. Several studies have addressed where and when T-cell MHC/peptide ligands are presented during viral and bacterial infections. For example, during *Listeria monocytogene*s infection, early antigen presentation was sufficient to drive the full program of CD8 T-cell expansion and contraction (8). Antigen presented by MHC-I and MHC-II proteins has been shown to persist following influenza and vesicular stomatitis virus infections (15, 44), and it likely is responsible for the maintenance of effector T-cell responses during chronic infections (52).

Ehrlichiosis is an emerging infectious disease of both humans and animals and is caused by obligate intracellular rickettsiae of the genus *Ehrlichia*. Our studies have focused on *Ehrlichia muris*, which first was identified in *Eothenomys kageus* mice in Japan and in *Hemaphysalis flava* ticks (47). Although the bacterium was discovered in mice, *E. muris* is closely related to ehrlichiae that cause human and animal diseases, in particular, *Ehrlichia chaffeensis*, the etiologic agent of human monocytotropic ehrlichiosis (32). Unlike *E. chaffeensis*, *E. muris* causes a low-level persistent infection in mice (31, 47). Moreover, *E. muris* infection generates protective immunity against another closely related but highly virulent ehrlichia, first identified in *Ixodes ovatus* ticks in Japan, known as ehrlichia from *Ixodes ovatus* (IOE) (37). It is not certain why *E. muris*, but not *E. chaffeensis* or low-dose IOE, can generate protective immunity against high-dose IOE infection. However, we have demonstrated that immunity to IOE can be achieved in the absence of classical CD4 T cell-mediated helper functions but not in the absence of B cells (4), suggesting that B cells and/or antibodies play a critical role in protective immunity. Nevertheless, CD4 T-cell responses are generated during infections by *E. muris* and other ehrlichiae and likely contribute to immunity, especially during chronic infection. For example, we have shown previously that CD4 T cells contribute to immunoglobulin class switching during *E. muris* infection, even though some class switching does occur in the absence of these cells (4).

In the present study, the display of MHC/peptide antigen

* Corresponding author. Mailing address: Wadsworth Center, 120 New Scotland Ave., Albany, NY 12208. Phone: (518) 473-2795. Fax: (518) 486-5592. E-mail: gary.winslow@wadsworth.org.

▽ Published ahead of print on 27 July 2009.

complexes in various tissues and anatomical locations has been monitored during acute and chronic *E. muris* infection. Our findings reveal that MHC-II/peptide antigen presentation and associated T-cell responses are regulated temporally and spatially during acute infection. Although dendritic cells (DCs) usually are considered the primary antigen-presenting cells (APCs) involved in antigen presentation to naive T cells (13, 28), the ehrlichiae are largely monocytotropic, and it was not known whether or when DCs harbor ehrlichiae and/or present MHC/peptide antigens to T cells. We show that CD11c-positive DCs harbor viable ehrlichiae and present specific antigen during the early phase of infection. Although chronic antigen presentation occurs in the peritoneal cavity and likely is responsible for chronic CD4 T-cell activation, the ehrlichiae nonetheless are able to avoid elimination while residing in macrophages. These findings have important implications for our understanding of how the ehrlichiae and related pathogens evade the cellular immune response during chronic infection.

MATERIALS AND METHODS

Mice. C57BL/6J mice were obtained from the Jackson Laboratories (Bar Harbor, ME) and were housed at the Wadsworth Center under microisolater conditions in accordance with institutional guidelines for animal welfare. In all studies, mice judged to be moribund were humanely euthanized.

Bacterial infections. Experimental intravenous inoculations were performed with aliquots of C57BL/6J spleen mononuclear cells that had been stored at −80°C, as described previously (4).

Generation of the T-cell line. The OMP-$19_{107\text{-}122}$-specific T-cell line was generated using T cells obtained from mice immunized with OMP-19, as described previously (26). The cells were cultured for 4 days with OMP-$19_{107\text{-}122}$ in complete tumor medium (CTM) (23) containing 10% fetal bovine serum (FBS), followed by 3 days without added peptide but with 20 U/ml of recombinant human interleukin-2 (IL-2). The cells then were cultured in medium without antigen or IL-2, and the cycle was repeated until a stable T-cell line was obtained. The cells were maintained in culture using the same protocol. To obtain cells for the direct ex vivo antigen detection (DEAD) assay, we harvested the T-cell line 3 days after antigen stimulation; aliquots were stored at −80°C in 7% dimethylsulfoxide (DMSO)–10% FBS. The cells were used in the DEAD assay immediately after being thawed. The OMP-$19_{107\text{-}12}$ peptide was described previously (26).

Antigen detection assay. The DEAD assay was performed essentially as described previously (2), except that the cells were used directly from frozen stocks, since we had determined that this step does not affect assay sensitivity. The $OMP_{107\text{-}122}$ T-cell line was labeled with carboxyfluorescein succinimidyl ester (CFSE; 5 μM), as described previously (34), and was cultured at a concentration of 1×10^6/ml in CTM in the presence of APCs obtained from various tissues. The APCs first were treated to eliminate erythrocytes, as described previously (5), and T cells were depleted from the APC preparations with an anti-CD4 antibody (HIO3.4), anti-CD8 (monoclonal antibody [MAb] 53.6), and rabbit complement. The APCs were cultured at a concentration of 1×10^6/ml in CTM plus 30 μg/ml brefeldin A with the T-cell line. After 5 h, the cells were harvested and surface stained for peridinin chlorophyll protein (PerCP)-conjugated CD4 (MAb RM4-5; BD Biosciences, Mountain View, CA); the cells then were fixed with 2% formaldehyde, permeabilized with 0.5% saponin (Sigma Chemical), and stained with allophycocyanin-conjugated anti-IFN-γ (MAb XMG1.2; BD Biosciences). The CFSE-labeled T cells were analyzed on a FACSCalibur flow cytometer, and the flow-cytometric data were analyzed by FlowJo software (Tree Star, Inc., Ashland, OR). The data in the figures were plotted after the subtraction of IFN-γ-producing cells detected in control samples that lacked specific antigen.

ELISpot assays. The number of antigen-specific CD4 T cells in spleens, lymph nodes (LN), and peritoneal exudate cells (PECs) was determined using a standard enzyme-linked immunospot (ELISpot) assay (24). The assays were performed in triplicate and used a starting concentration of 1×10^6 cell/ml (100 μl/well) purified CD4 T cells, which were serially diluted. The cultures contained, in addition, 1×10^6 spleen APCs. The assays were performed using recombinant OMP-19, which has been described previously (26), at a concentration of 10 μg/ml. Specific responses were quantitated by subtracting the number of spots, if any, detected in the absence of the specific antigen, or using an irrelevant antigen. The latter was the West Nile virus NS5 methyl transferase protein that was generated, purified, and used in the same manner as OMP-19 (54) (kindly provided by Hongmin Li, Wadsworth Center). Spots were enumerated by visual inspection using a stereo microscope (Olympus SZ61).

Flow cytometry. For the detection of T cells in peritoneal exudates, cells were harvested by lavage and stained with PerCP-conjugated anti-CD8 (MAb 53.6), allophycocyanin- or PerCP-conjugated anti-CD4 (MAb SK3 and RM4-5, respectively), and phycoerythrin (PE)-conjugated anti-CD69 (MAb H1.2F3), all obtained from BD Biosciences. Allophycocyanin-conjugated anti-KLRG1 (MAb 2F1) was obtained from eBiosciences. Data were acquired on a FACSCalibur flow cytometer equipped with CellQuest software (BD Biosciences) and were analyzed with FlowJo software (Tree Star, Inc.).

DC purification and depletion. Following T-cell depletion, DCs were purified from infected spleens and LNs by magnetic bead positive selection using CD11c-conjugated microbeads (Miltenyi Biotec) by following the protocol supplied by the manufacturer. Purification was performed manually. The DCs then were stained with PE-conjugated anti-IA^b (MAb AF6-120.1; BD Biosciences) and APC-conjugated anti-CD11c (MAb HL3; BD Biosciences), and the cells were further purified using a FACSAria cell sorter (BD Biosciences). DC-depleted spleen cells were obtained on day 8 postinfection by harvesting the eluate from the CD11c magnetic bead column after two successive separations.

Imaging. For the detection of cells and bacteria in situ, spleens were embedded in Neg-50 medium (Richard-Allan Scientific, Kalamazoo, MI), frozen on dry ice, and stored at −80°C. Cryostat sections (7 μm) were fixed in ice-cold acetone for 15 min and rehydrated in phosphate-buffered saline (PBS). To block nonspecific binding, the sections were treated for 30 min at 37°C with Fc blocking solution containing 10% normal rabbit serum. The sections were stained in succession with rat anti-mouse MOMA-1 (overnight; Serotec, Raleigh, NC), biotinylated rabbit anti-rat immunoglobulin G (60 min at room temperature [RT]; Vector Laboratories, Burlingame, CA), and streptavidin-Alexafluor-350 (30 min; Invitrogen, Carlsbad, CA); the sections then were washed extensively in PBS and blocked with 2% bovine serum albumin (BSA) for 60 min at RT. The sections next were incubated with biotinylated hamster anti-mouse CD11c (1 h at RT; BD Biosciences) and streptavidin-Alexafluor-647 (30 min; Invitrogen, Carlsbad, CA). For the detection of *E. muris*, biotinylated Ec18.1 (1 h at RT) (18) and streptavidin-Alexafluor-488 (30 min; Invitrogen, Carlsbad, CA) were used. When biotinylated antibodies were used, a streptavidin-biotin blocking kit (Vector Laboratories, Burlingame, CA) was applied between each of the successive antibody incubations. The stained sections were mounted in antifading reagent (Slow Fade Gold; Invitrogen, Carlsbad, CA). Images were acquired with an epifluorescence microscope (Azioskop2; Carl Zeiss SMT, Peabody, MA) equipped with a Hamamatsu camera and were processed using OPENLAB software (Zeiss).

For the detection of *E. muris* in flow-cytometrically sorted DCs, the cells were centrifuged onto poly-L-lysine-coated cytospin slides (Shandon Cytospin), fixed in 1% paraformaldehyde (20 min RT), and blocked with 2% BSA (1 h at RT). The cells were stained with biotinylated hamster anti-mouse CD11c (1 h at RT; BD Biosciences) followed by streptavidin-Alexafluor-647 (30 min; Invitrogen). The cells were washed in PBS and blocked with PBS containing 5% FBS (20 min at RT). For the detection of extracellular bacteria, the cells were incubated with biotinylated Ec18.1 for 1 h at RT, followed by incubation with streptavidin-Alexafluor 594 (Invitrogen) for 30 min. For the detection of intracellular bacteria, the same cells as those described above were washed in PBS and incubated for 20 min with 5% FBS containing 0.2% saponin (1). The saponin-permeabilized cells were incubated with biotinylated Ec18.1 for 1 h at RT, followed by incubation with streptavidin-Alexafluor-488 (Invitrogen) for 30 min. Since all of the antibodies used in this staining procedure were biotinylated, a streptavidin-biotin blocking kit (Vector Laboratories, Burlingame, CA) was used between successive antibody incubations. The cells were mounted and analyzed in the same medium as that described above. For the detection of bacteria within peritoneal macrophages, the cells were stained with fluorescein isothiocyanate-F4/80 (Serotec) and biotinylated Ec18.1.

Statistical analyses. The statistical analyses were performed by use of a one-tailed Mann-Whitney test with a confidence interval of 99%. The data were analyzed with Prism software (GraphPad Software, Inc.).

RESULTS

Detection of OMP-19 T-cell antigen presentation during *E. muris* infection. To determine the role of antigen in the generation and maintenance of CD4 T-cell responses, we have

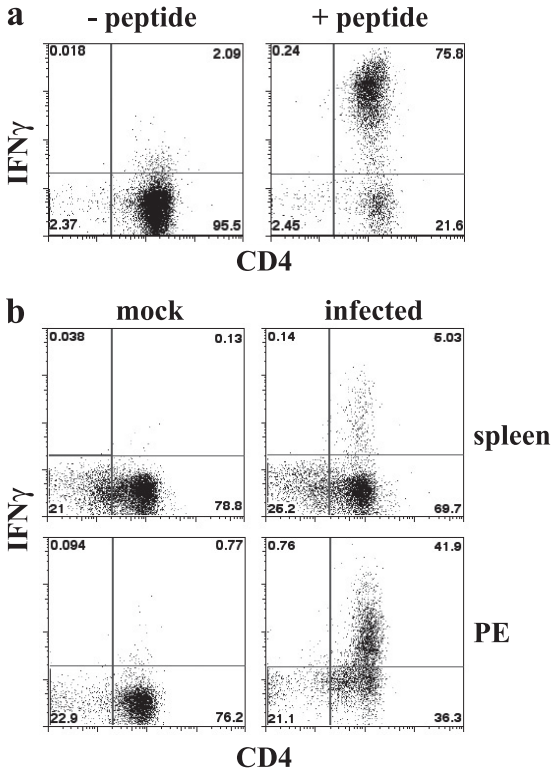

FIG. 1. Detection of IA^b/OMP-$19_{107-122}$ antigen presentation. T-cell-depleted APCs were incubated with the OMP-$19_{107-122}$-specific CD4 T-cell clone for 5 h in the presence of brefeldin A, and the T cells then were stained for intracellular IFN-γ. The T-cell clone was labeled with CFSE, and the CFSE-negative APCs were excluded from the flow cytometry analyses. (a) Uninfected T-cell-depleted spleen APCs (1×10^6) were incubated with the T-cell clone in the absence or presence of OMP-$19_{107-122}$. (b) Either T-cell-depleted spleen cells or PECs from a mock-infected or day 12-infected mice were incubated with the OMP-$19_{107-122}$ T-cell line, as described for panel a. The data in panel b are representative of data obtained from three mice.

evaluated the anatomical location(s) of T-cell MHC/peptide antigen display by APCs during acute and chronic *E. muris* infection. Although the detection of MHC/peptide antigen complexes has been addressed using monoclonal antibodies specific for such complexes (14), these reagents often lack the sensitivity available from bioassays. Accordingly, we have used the DEAD assay originally described by Badovinac and colleagues (2). A particular advantage of this approach is that the detection of MHC/peptide antigens displayed on the surface of APCs by activated in vitro-cultivated T-cell lines does not require T-cell costimulatory signals; thus, the assay uses the responding cells to provide a relatively unbiased detection of MHC/peptide antigens on APCs. For our studies, a T-cell line was generated that responded to *E. muris* OMP-$19_{107-122}$, an MHC-II/peptide antigen identified in our previous study (26). The T cells responded to IA^b/OMP-$19_{107-122}$ presented by T cell-depleted C57BL/6 spleen APCs by producing IFN-γ (Fig. 1a). The T-cell line also detected IA^b/OMP-$19_{107-122}$ on the surface of T-cell-depleted spleen APCs and PECs obtained from C57BL/6 mice 12 days after intravenous inoculation with 5×10^4 bacteria (Fig. 1b). In this experiment, approximately 6.5 and 52.6% of the CD4-positive T cells in the spleen and PEC cultures, respectively, detected MHC/peptide complexes. Not all of the T cells in the culture responded, probably because the MHC/peptide was present on only some of the cells from the infected mice. Differences in the magnitude of the T-cell response between spleen and PECs likely reflect differences in cell composition (i.e., the percentage of APCs) in the cultures, as well as the density of MHC/peptide complexes on the APCs. Thus, the DEAD assay provides an overall measure of MHC/peptide antigen display within a particular tissue during infection.

The experimental strategy described above was used to quantitate the frequency of IFN-γ-producing T cells that responded to IA^b/OMP-$19_{107-122}$ at various times after intravenous *E. muris* infection in spleen, LNs (pooled brachial, axillary, and inguinal LNs), and PECs (Fig. 2a). IA^b/OMP-$19_{107-122}$ presentation was detected within 5 days postinfection in spleen, and it reached a maximum on day 6 postinfection. In LNs, IA^b/OMP-$19_{107-122}$ was detected as early as 5 days postinfection, but presentation did not reach a maximum until day 16 postinfection; by day 21, LN antigen presentation was largely undetectable. In PECs, antigen presentation began on day 12 postinfection, was maximal on day 16, and stabilized at relatively high levels for at least as long as 60 days postinfection.

Although the above-described assays were performed by sampling the same number of cells from each of the organs and from preparations of PECs, the cellularity of the spleen and peritoneal cavity clearly was altered following intravenous infection (Fig. 2b). Similarly to our previous observations after intraperitoneal *E. muris* inoculation, infection in the present study was accompanied by massive splenomegaly and an increase in peritoneal cavity cellularity following intravenous infection. In the spleen, antigen presentation, on a per-cell basis, declined during the time period that tissue cellularity was increasing. In the peritoneal cavity, the apparent sudden increase in antigen presentation on day 12 postinfection also may reflect changes in cell composition, given that we observed a large increase in the frequency of $CD11b^{hi}$ F4/80-positive macrophages on day 12 postinfection (see below). We can conclude, nevertheless, that the relative frequencies of IA^b/OMP-$19_{107-122}$ APCs undergo dynamic temporal and spatial changes during *E. muris* infection.

Overall, the changes in antigen presentation were reflected by changes in bacterial colonization in the tissues, suggesting a causal relationship (Fig. 2a and c). To directly address a possible relationship between infection and IA^b/OMP-$19_{107-122}$ presentation, we performed the DEAD assay with spleen cells and PECs from mice on day 60 postinfection, after the mice had been treated three times (on days 50, 54, and 57 postinfection) with doxycycline, an antibiotic known to be effective against the ehrlichiae (6, 21). Antibiotic treatment reduced antigen presentation by approximately twofold in each assay (Fig. 2d), and this reduction was correlated with a reduction in *E. muris* infection (Fig. 2e). The data also reveal that, although doxycycline is highly effective in treating ehrlichiosis, a significant proportion of the bacteria in the mouse peritoneal cavity appeared to be refractory to antibiotic treatment.

Effector CD4 T cells accumulate at sites of antigen presentation during acute and chronic infection. We next addressed whether IA^b/OMP-$19_{107-122}$-specific CD4 T-cell effector responses in vivo correlated with antigen presentation by per-

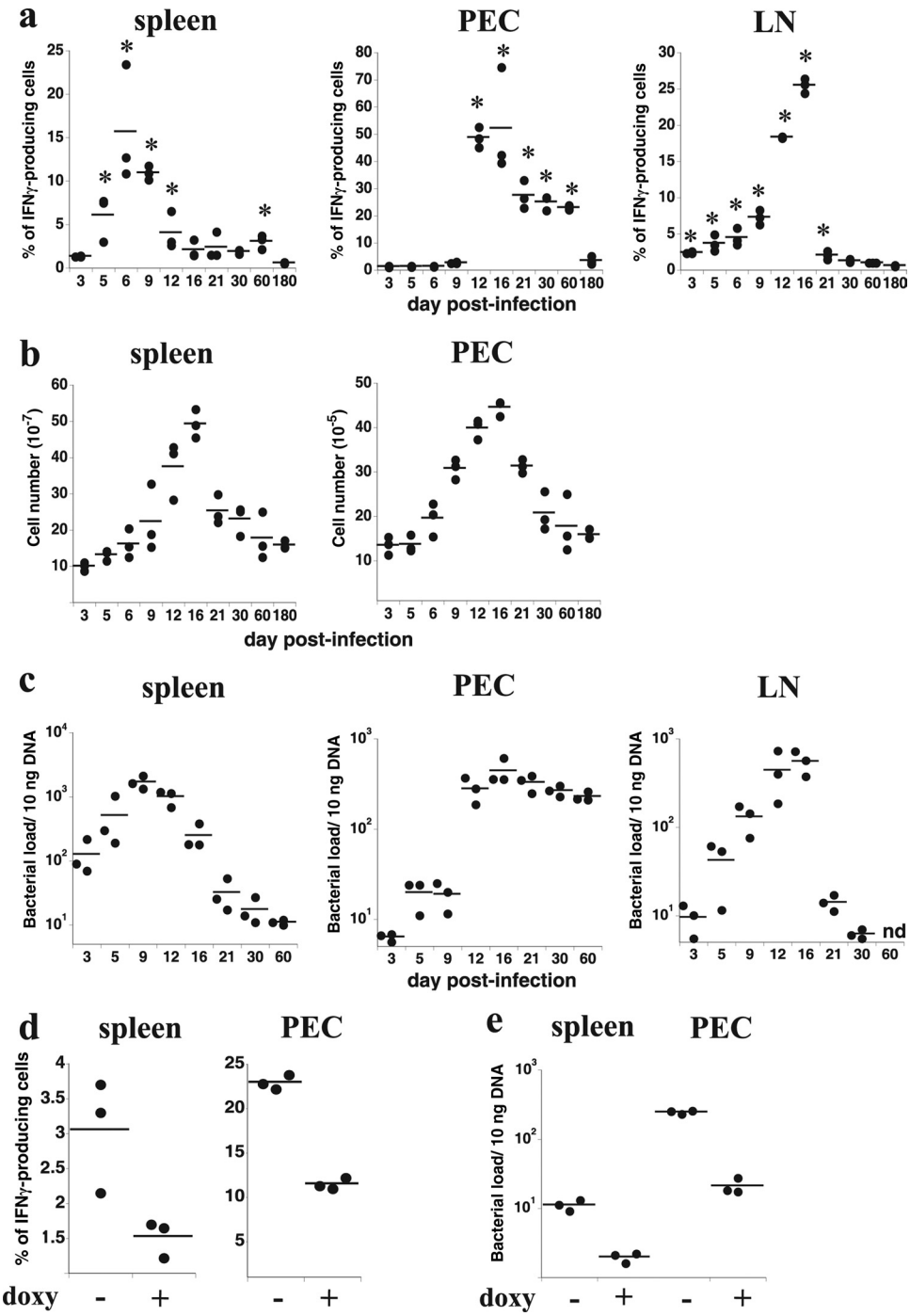

FIG. 2. MHC/peptide antigen display during *E. muris* infection. Antigen presentation, tissue cellularity, bacterial infection, and the effects of antibiotic treatment were measured in the indicated tissues and anatomical locations after intravenous ehrlichial infection with 5×10^4 bacteria. (a) T-cell-depleted APCs from spleen, within PECs, and pooled brachial, axillary, and inguinal LNs (1×10^6 cells each) were analyzed for OMP-$19_{107\text{-}122}$ antigen presentation on the indicated days postinfection using the approach described in the legend to Fig. 1. Each datum represents the determination from a single mouse. The data were compiled from several different infections. Horizontal lines indicate the mean values. The asterisks indicate statistically significant differences in values relative to the values of uninfected control APCs, as determined using the Mann-Whitney test ($P < 0.05$). The data were plotted after subtracting the background level obtained using uninfected control APCs. (b) Total spleen and peritoneal cavity mononuclear cell numbers were determined on the indicated days postinfection. (c) Bacterial copy numbers (per 10 ng of tissue DNA) were determined on the indicated days postinfection. (d) Mice were untreated or were administered doxycycline (doxy; 400 μg) on days 50, 54, and 57 postinfection, and ex vivo antigen presentation by spleen and peritoneal APCs was measured on day 60 postinfection. (e) Bacterial infection was measured in the mice analyzed in panel d. The experiment described for panels d and e was performed once. nd, not determined.

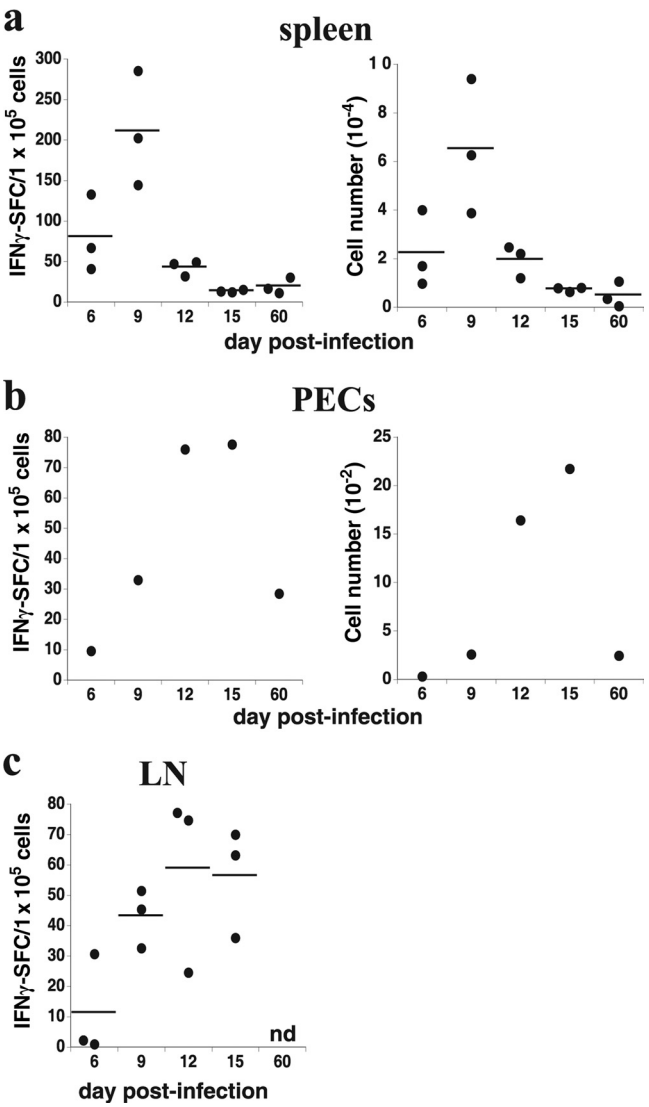

FIG. 3. Kinetics of the effector CD4 T-cell response during infection. (a to c) CD4 T cells were purified from infected mice by magnetic bead negative selection and were incubated for 48 h with uninfected spleen APCs in the presence of recombinant OMP-19 (10 μg/ml). ELISpot analyses for IFN-γ were performed, and the frequency and number of spot-forming cells (SFCs) in the indicated tissues were determined (left and right panels, respectively). Each datum represents a determination from a single mouse, and horizontal lines indicate the mean values, except for the peritoneal cavity analyses (b), where the data represent the frequency and number of SFCs identified in pooled peritoneal lavage from three mice at each time point. n.d., not determined. All of the values obtained in cultures from the infected mice were statistically different from results of control assays, which were performed in the absence of OMP-19, or using an identically prepared irrelevant antigen (not shown). SFCs detected in wells that lacked peptide were negligible and were subtracted from the experimental samples. Very similar results were obtained using intraperitoneal infections in several related experiments.

forming IFN-γ ELISpot analyses. Antigen presentation was a good predictor of effector CD4 T-cell responses; the frequency and number of ex vivo IFN-γ-producing CD4 T cells in the various mouse tissues correlated with tissue antigen presentation (compare Fig. 3 to 2a). We also addressed whether antigen presentation in the peritoneal cavity was associated with an influx of polyclonal populations of T cells. Both CD4 and CD8 T cells were detected at high frequencies, relative to the frequencies in normal mice, during peak antigen presentation on day 12 postinfection (29.4 and 14.5%, respectively) (Fig. 4a and b). The frequencies and numbers of CD4 and CD8 T cells remained at least twofold higher than those in normal mice for as long as 60 days postinfection, a finding also consistent with the idea that persistent antigen presentation is occurring in the peritoneal cavity at this time.

These data also revealed that CD4 T cells reside in the peritoneal cavity during chronic *E. muris* infection in the presence of ehrlichial MHC/peptide antigens. Chronic antigen exposure can lead to terminal differentiation and/or the exhaustion of T cells (51). To examine whether the peritoneal CD4 T cells exhibited characteristics of chronically activated effector cells, the T cells were evaluated for the surface expression of the activation marker CD69 (17, 45) and for the killer cell lectin-like receptor G1 (KLRG1), an inhibitory receptor originally identified on NK cells (22). KLRG1 expression has been associated with nonproliferative senescence in T cells (46), and stimulation with persistent antigen has been shown to increase KLRG1 expression on virus-specific CD8 T cells (42). More than 50% of the polyclonal population of CD4 T cells detected within the peritoneal cavity on day 60 after *E. muris* infection expressed CD69, and 25% of CD4 T cells expressed KLRG-1 (a 10- and 5-fold increase compared to the levels for uninfected mice) (Fig. 4c). These data reveal that *E. muris* can persist even in the presence of displayed antigen and terminally differentiated CD4 T cells, suggesting that infected host APCs are refractory to T-cell-derived signals during chronic infection.

DCs are highly effective APCs and harbor *E. muris* in vivo. DCs are well known to be the major APCs that trigger naive T-cell responses, although such a function for DCs has not been formally demonstrated following ehrlichial infection. Moreover, the ehrlichiae are considered to be largely monocytotropic, and it had not been known whether DCs are actual targets of infection or whether they phagocytose bacteria or bacterial antigens to present them to CD4 T cells. To address whether DCs present ehrlichial MHC/peptide antigens, we purified day 5 postinfection spleen and LN DCs using CD11c-mediated magnetic bead positive selection and flow-cytometric cell sorting (Fig. 5a). The day 5 postinfection time point was chosen because this was when IA^b/OMP-$19_{107-122}$ was first detected in the spleen. The purified DCs (>96% CD11c positive) were highly efficient at presenting IA^b/OMP-$19_{107-122}$ (Fig. 5b). Antigen presentation was considerably more efficient in spleen cultures than in LN cultures: 50.4 and 13.0% of the CD4 T cells responded, respectively. The differences between the two cultures likely reflected organ-specific temporal changes in antigen presentation observed during infection (Fig. 1). To address the extent to which DCs contributed to spleen antigen presentation in early ehrlichial infection, DCs were depleted using two rounds of CD11c-mediated magnetic bead negative selection; the remaining APCs (containing less than 0.1% DCs) were used in antigen presentation assays. The depletion of DCs from day 6-infected spleens in three experiments reduced antigen presentation by 56, 62, and 80%, respectively. These data reveal that DCs constitute a major APC

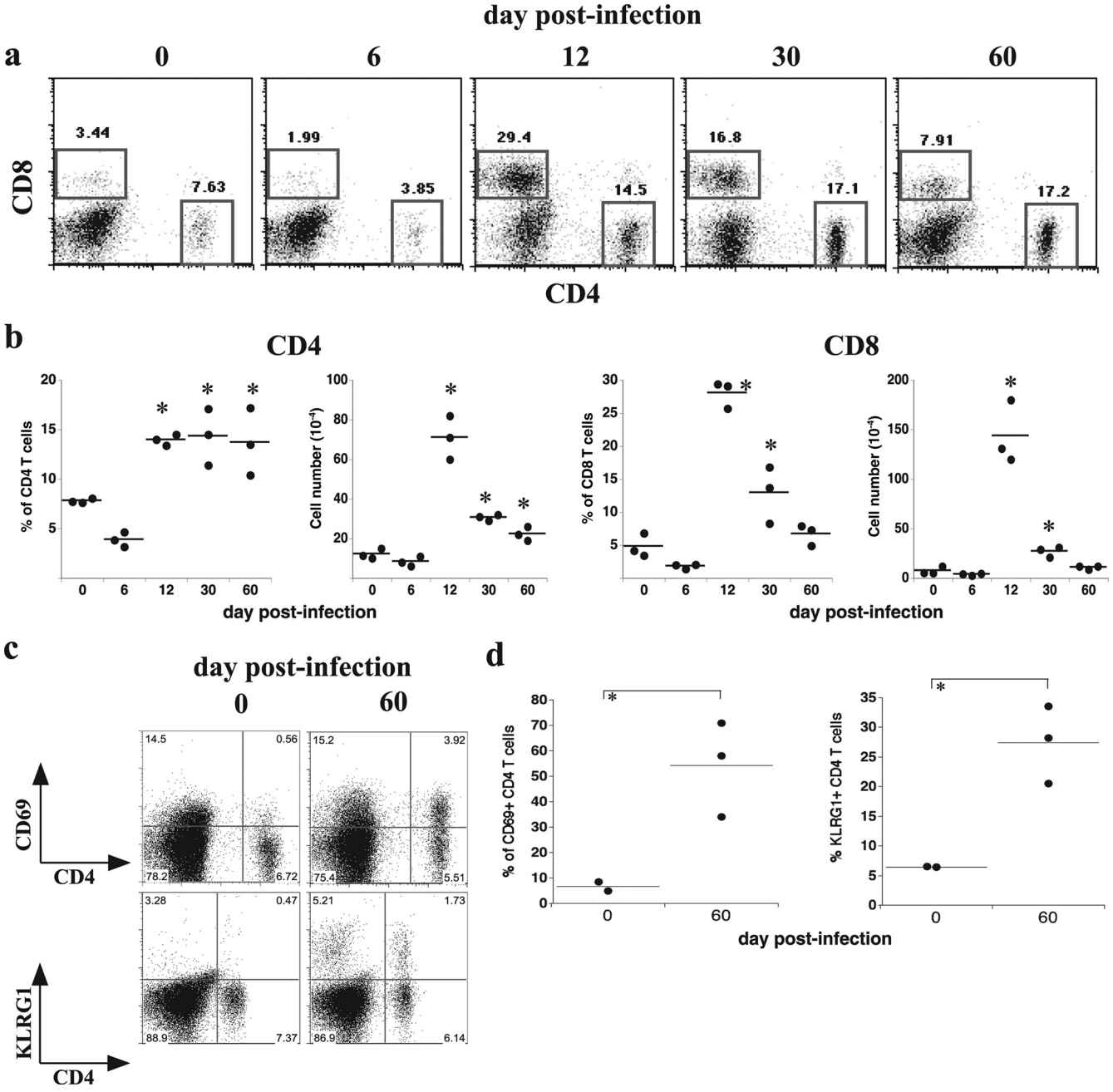

FIG. 4. T-cell expansion and persistence in the peritoneal cavity during acute and chronic infection. PECs were isolated by lavage and were analyzed for the presence of CD4 and CD8 T cells on the indicated days postinfection by flow cytometry. (a) Representative dot plots are shown; the analyses were performed after flow cytometric gating on viable cells. (b) The frequencies and numbers of CD4 and CD8 T cells detected in each of the mice analyzed in panel a are shown. An asterisk indicates a statistically significant difference in value, relative to the value of day 0 control samples, determined using the Mann-Whitney test ($P < 0.05$). The experiment was performed two times. (c) A representative flow cytometric analysis of surface expression of CD69 and KLRG1 on CD4 T cells obtained from the peritoneal cavity on day 60 postinfection and an aged-matched control mouse is shown. (d) The frequencies of CD4 T cells that expressed the markers analyzed in panel c are shown in the graphs.

population in the spleen 6 days after *E. muris* infection, although it is not the only one.

Although DCs clearly presented IA^b/OMP-$19_{107-122}$, this could have been the result of direct infection and/or the indirect capture of antigen, possibly via cross-antigen presentation (11). To determine whether DCs harbored bacteria in vivo, we purified DCs from spleens on day 5 postinfection by CD11c magnetic bead selection followed by flow-cytometric cell sorting; the cells then were stained with an anti-OMP-19 monoclonal antibody that recognizes *E. muris* (Ec18.1) (19). To distinguish between intracellular and cell-associated bacteria, we performed immunochemical staining prior to and after

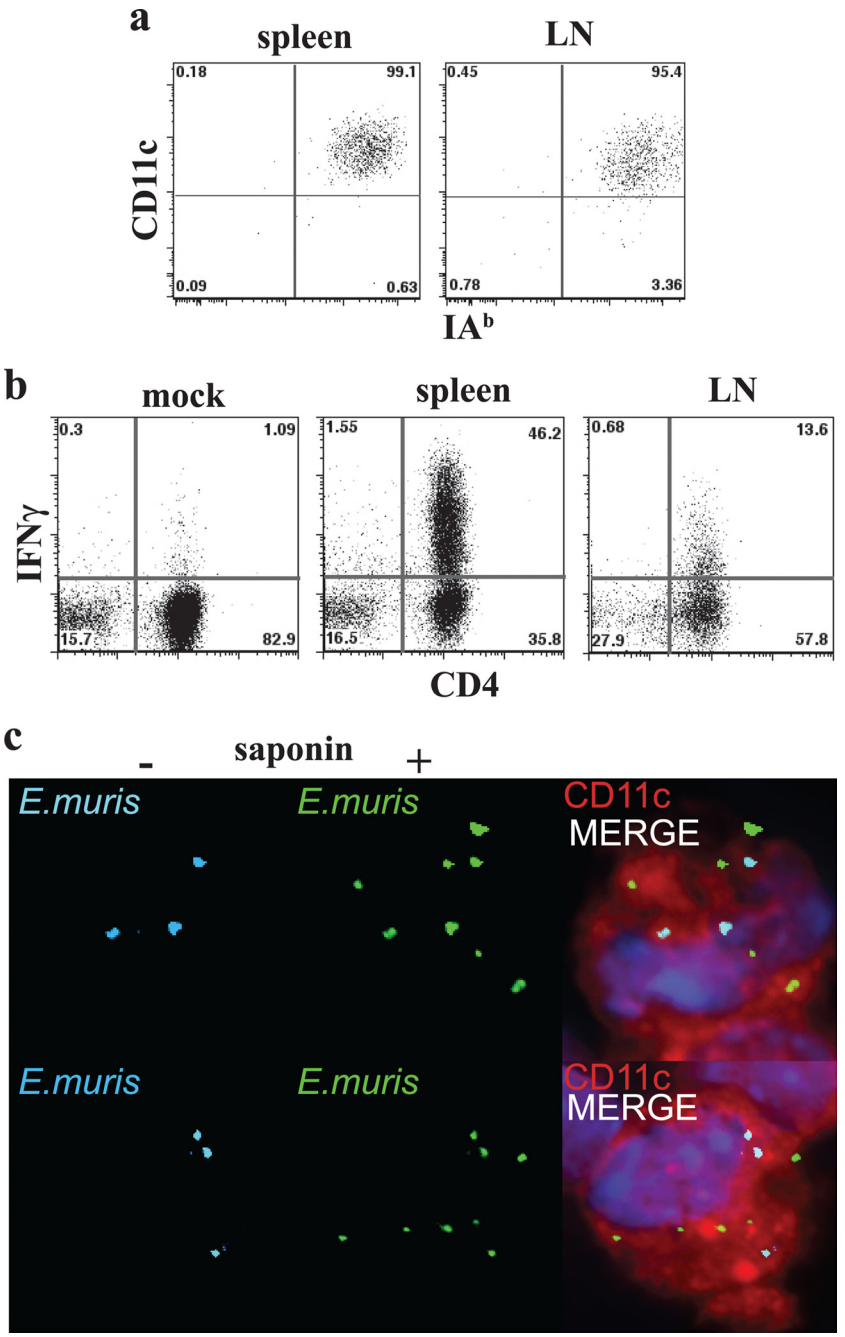

FIG. 5. DCs display antigen and harbor *E. muris*. DCs were purified from pooled day 5-infected spleens and LNs ($n = 3$), enriched by magnetic bead positive selection, and then purified by flow-cytometric cell sorting (95 to 99% purity was obtained). (a) Representative dot plots demonstrating the homogeneity of each of the purified DC populations. (b) OMP-$19_{107\text{-}122}$ antigen presentation was measured in cultures containing the DCs, purified as described for panel a, from mock-infected mice (mock) or from spleen and LNs from mice on day 5 postinfection. The data are representative of two independent experiments of similar design; the average frequencies of IFN-γ-producing T cells were 43.7 and 13.6% for spleen and LNs, respectively. (c) DCs from mice on day 5 postinfection were purified by flow-cytometric cell sorting as shown in panel a and were stained with antibodies that recognize *E. muris* (Ec18.1) and CD11c. The staining for *E. muris* was performed using biotinylated Ec18.1. The cells first were stained using streptavidin-conjugated Alexafluor-594 (pseudocolored cyan in the figure), permeabilized with 0.2% saponin, blocked, and stained again with streptavidin-conjugated Alexafluor-488 (shown in green). Thus, the cyan-colored bacteria are surface-associated bacteria, and the green bacteria represent all of the bacteria associated with the host cell. The merged image, which also includes CD11c staining (in red), is shown in the panels at the right. Nuclei were counterstained with 4′,6′-diamidino-2-phenylindole (blue in nuclei). The top and bottom rows show two representative fields of cells.

saponin treatment using distinct secondary reagents to detect the external and internal bacteria. *E. muris* was detected within the spleen DCs, indicating that the DCs either phagocytosed the bacteria or were actively infected (Fig. 5c). Approximately 23% of the spleen CD11c-positive DCs harbored one or more *E. muris* morulae ($n = 199$); most of the infected DCs contained 1 to 3 morulae per cell (range, 1 to 10). Many of the ehrlichiae were detected inside the DCs (range, 33 to 66%),

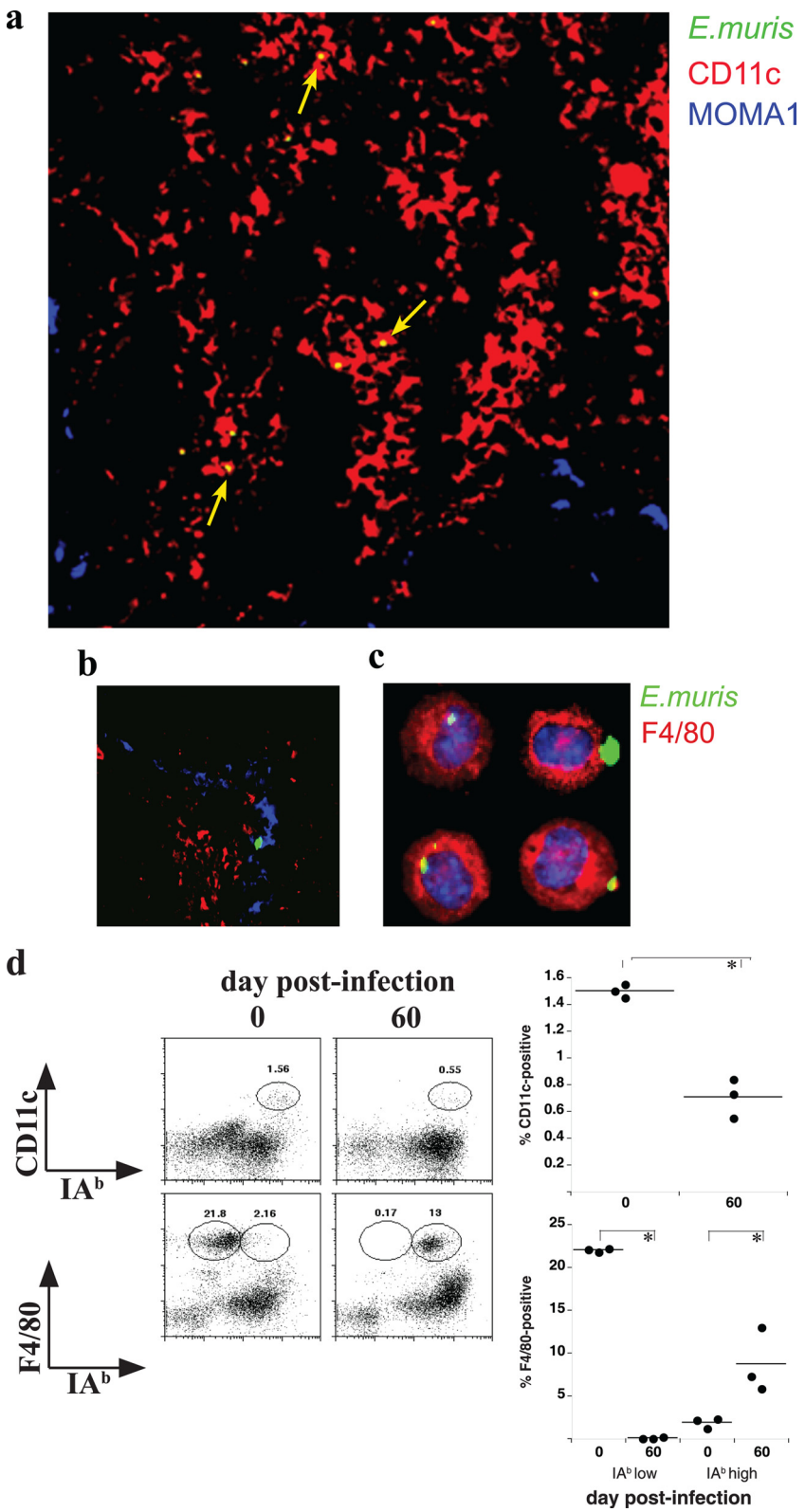

FIG. 6. *E. muris* infection of APCs in situ. Spleen tissue was harvested from a mouse on day 6 postinfection, sectioned, and stained using the antibodies described in the legend to Fig. 5c and MOMA-1, which recognizes MZ metallophilic macrophages. (a) A representative merged image of a portion of a spleen is shown. CD11c staining is shown in red, and MOMA-1-positive macrophages are shown in blue. The bacteria were stained with biotinylated Ec18.1 and streptavidin-conjugated Alexafluor-488; these were imaged as green but appear yellow in the merged panel, because they are present in the red CD11c-positive DCs (yellow arrows). (b) Representative image from a portion of a spleen section showing bacteria residing in MOMA-1-positive macrophages (blue arrows). (c) PECs were isolated from a mouse on day 30 postinfection, and the cells were stained

although a relatively large portion of bacteria were found on the cell surface. The significance of the DC surface-associated bacteria is not known, but surface presentation may facilitate the recognition of the bacteria by B cells (3, 20).

To address whether the bacteria associated with the DCs were intact and infectious, DCs were obtained from *E. muris*-infected mice on day 5 postinfection and purified by flow cytometry (as described for Fig. 5a), and 0.5×10^6 cells were transferred to uninfected C57BL/6 mice. On day 8 after transfer, the recipient mice harbored an average of 1.3×10^3 bacteria per 10 ng of spleen DNA and exhibited characteristically large spleens (data not shown), indicating that the DCs indeed harbored infectious bacteria. To localize *E. muris*-infected DCs in vivo, spleen tissue from day 6-infected mice was stained with anti-CD11c, as well as an antibody that recognizes marginal metallophilic macrophages (MOMA-1) and Ec18.1. MOMA-1 was used to delineate the marginal zone (MZ) and spleen follicles. Most of the infected cells detected at this time were located outside of the B-cell follicles and MZ, in the red pulp (68%); the majority of the bacteria colocalized with or were closely associated with CD11c-positive DCs (57%; $n = 129$ infected cells) (Fig. 6a). Some bacteria were detected in non-DCs, including MOMA-1-positive macrophages (12%) (Fig. 6b); this finding suggests a role for MOMA-1 macrophages in bacterial phagocytosis and/or antigen presentation. The remaining 20% of the bacteria were detected within the white pulp. These data confirm that both DCs and macrophages harbor *E. muris* and likely display MHC/peptide antigens during the early stages following intravenous infection.

Because antigen presentation persisted in the peritoneal cavity, we also investigated which APCs were present and infected during chronic infection at this location. On day 30 postinfection, bacteria were found to be colocalized nearly exclusively with F4/80-positive macrophages (Fig. 6c). Approximately 10% of the F4/80 macrophages were infected, and the bacteria were found only in these cells. Moreover, F4/80-positive macrophages were the predominant APC detected within the peritoneum; while class II IA^b was expressed by only a small proportion of macrophages in uninfected mice, nearly all of the macrophages from infected mice expressed large amounts of the MHC protein (Fig. 6d). However, as some DCs also are present in the peritoneal cavity during chronic infection, we cannot yet conclude if macrophages actually are responsible for presenting antigen to T cells APC.

DISCUSSION

Our data reveal a strikingly dynamic process of infection and antigen display during both acute and chronic phases of ehrlichial infection following intravenous inoculation. The spleen was the site where the majority of MHC/peptide complexes were detected early after infection, presumably reflecting the rapid sequestration of blood-borne organisms in this tissue. Thus, the spleen is likely the major site of T-cell priming during blood-borne ehrlichial infections. Given that DCs are well known to be the most efficient cell type in the activation of T cells and that macrophages are poor activators of naive T cells (35), these data also suggest that CD4 T cells first are primed in the spleen by DCs early following infection. The ehrlichiae generally are considered monocytotropic, although some species have been shown to infect endothelial cells and hepatocytes (39). Our data reveal, in addition, that DCs are targets of ehrlichial infection, as the transfer of DCs from infected mice led to the bacterial colonization of naive mice. Thus, our data suggest that DCs can serve as host cells for ehrlichial infection in vivo, as has been shown to occur for other intracellular bacterial infections (9, 12, 27, 41). It is not known whether or how the requirements for the colonization of DCs differs from macrophage colonization, or whether DC infection is transient or persistent. It also is possible that blood-borne DCs become infected and transfer the ehrlichiae to the spleen, as has been suggested to occur during *Listeria monocytogenes* infection (27). The significance of the DC surface-associated bacteria also is not known, although one possibility is that bacteria or bacterial antigens so presented are available for recognition by B cells (3).

Although we detected some peptide/MHC antigens in LNs early after infection, maximal antigen presentation in the LNs did not occur until day 16 postinfection, a time point when spleen antigen presentation had declined rather precipitously. This observation that the timing of antigen display varies with anatomical location suggests that naive T cells undergo priming sequentially at these various sites. Because the type and quality of DCs in spleen and LNs differ (38), the anatomical context wherein T cells encounter antigen may result in qualitatively distinct T-cell responses during infection. The marked changes in the timing and anatomical localization of antigen presentation during ehrlichial infection are at least partly driven by bacterial tissue tropism, given that infection and antigen presentation were closely linked. Such linkage need not necessarily occur, as during influenza infection it has been demonstrated that CD4 T-cell antigen presentation persisted in the absence of viral infection (15). The factors that govern the spread of the blood-borne bacteria are not known, however. The relatively late presentation and infection in LNs may indicate that the bacteria gain access to the lymph more slowly, perhaps within infected monocytes that must traverse endothelial barriers. The manner whereby the bacteria spread throughout the body (i.e., in blood and/or lymph) is not well understood and deserves more investigation.

Antigen display by the PECs occurred abruptly, between days 9 and 12 postinfection, and in contrast to that of spleen and LN, presentation persisted for at least 60 days in the peritoneal cavity. Although antigen presentation appeared

using fluorescein isothiocyanate-conjugated F4/80 (pseudocolored in red) and biotinylated Ec18.1, followed by Alexafluor-647 (pseudocolored in green). Nuclei were stained with 4′,6′-diamidino-2-phenylindole; the large green structures containing the fluorescent bacteria are morulae. (d) PECs from day 60 postinfection and age-matched control mice were monitored by flow cytometry for the surface expression of CD11c and F4/80 on class II IA^b-positive and -negative cells (left). The percentages of the gated populations within the live cell gate are shown in each plot. The right panels show the frequencies of CD11c- and F4/80-positive cells in the indicated populations from each of the mice analyzed.

to be most robust in the PECs, this finding likely reflects the abundance of infected APCs in the peritoneal cavity relative to that of the spleen and LNs. Indeed, we detected bacteria in or associated with approximately 10% of F4/80-positive peritoneal macrophages during chronic infection, and flow cytometry studies revealed that these were the major APCs detected in this anatomical location. Thus, PECs are a potent source of both APCs and specific antigen during chronic ehrlichial infection. Additional studies will be required to address whether persistent *E. muris* infection at other anatomical locations (i.e., liver and lung) (31) also contribute to long-lived antigen presentation and chronic T-cell responses.

While all of the studies described here utilized intravenous infection, we have obtained similar data after performing intraperitoneal infection; the only difference we observed using the different inoculation strategies was that antigen presentation occurred earlier in PECs following intraperitoneal inoculation (B. Nandi, M. Chatterjee, and G. Winslow, unpublished data). It is likely that the route of natural infection influences the kinetics and the sites of antigen presentation. During natural infection via tick transmission, infection and, perhaps, antigen presentation may be confined to peripheral tissues and draining LNs (10, 40). Further studies will be required to address possible differences in antigen presentation and immune responses between tick transmission and intravenous inoculation.

Why are the CD4 T cells found in the peritoneal cavity unable to clear chronic infection? Our data clearly demonstrate that the bacteria do not evade the immune response by inhibiting MHC-II antigen presentation, assuming that the studies of OMP-19 antigen presentation can be generalized to other T-cell antigens. An alternative explanation is that the ehrlichiae subvert the host defenses mounted by activated macrophages. Indeed, the CD4 T cells in the peritoneal cavity exhibit a phenotype that is characteristic of highly activated terminally differentiated nondividing effector T cells. Although a large proportion (25%) of the polyclonal CD4 T-cell population expressed the inhibitory receptor KLRG1, the T cells could produce IFN-γ ex vivo and likely were responsible for macrophage activation, as nearly all of the peritoneal macrophages exhibited high surface expression of MHC-II proteins during chronic infection. Thus, rather than suppressing T- and B-cell responses, the ehrlichiae instead appear to use macrophage-intrinsic mechanisms to subvert host defenses during chronic infection. Such mechanisms in macrophages likely include the inhibition of the production of reactive oxygen intermediates, phagosome-lysosome fusion, and IFN signaling, all mechanisms that have been documented in vitro for the ehrlichiae (36, 53). Thus, although the products of CD4 T cells may help to limit acute infection, activated T cells appear to be incapable of eliminating the bacteria once the bacteria have established chronic infection in macrophages. Similar conclusions have been drawn regarding CD4 T-cell immunity during chronic tuberculosis infection in the mouse (16, 43). Thus, the explanations for bacterial persistence are relevant not only to the ehrlichiae but also to other bacteria that establish chronic infections (25).

ACKNOWLEDGMENTS

We thank Robert Clark (University of Connecticut Health Sciences Center) for advice regarding the generation of the OMP-19-specific T-cell line, William Reiley of the Trudeau Institute for the critical reading of the manuscript, and the Wadsworth Center Immunology Core Facility.

This work was supported by U.S. Public Health Service grant R01AI64678 to G.M.W.

REFERENCES

1. **Agerer, F., S. Waeckerle, and C. R. Hauck.** 2004. Microscopic quantification of bacterial invasion by a novel antibody-independent staining method. J. Microbiol. Methods **59:**23–32.
2. **Badovinac, V. P., B. B. Porter, and J. T. Harty.** 2002. Programmed contraction of CD8$^+$ T cells after infection. Nat. Immunol. **3:**619–626.
3. **Balázs, M., F. Martin, T. Zhou, and J. Kearney.** 2002. Blood dendritic cells interact with splenic marginal zone B cells to initiate T-independent immune responses. Immunity **17:**341–352.
4. **Bitsaktsis, C., B. Nandi, R. Racine, K. C. MacNamara, and G. Winslow.** 2007. T cell-independent humoral immunity is sufficient for protection against fatal intracellular ehrlichia infection. Infect. Immun. **75:**4933–4941.
5. **Bitsaktsis, C., and G. Winslow.** 2006. Fatal recall responses mediated by CD8 T cells during intracellular bacteria infection. J. Immunol. **177:**4644–4651.
6. **Brouqui, P., and D. Raoult.** 1992. In vitro antibiotic susceptibility of the newly recognized agent of ehrlichiosis in humans, *Ehrlichia chaffeensis*. Antimicrob. Agents Chemother. **36:**2799–2803.
7. **Cheminay, C., A. Mohlenbrink, and M. Hensel.** 2005. Intracellular Salmonella inhibit antigen presentation by dendritic cells. J. Immunol. **174:**2892–2899.
8. **Corbin, G. A., and J. T. Harty.** 2004. Duration of infection and antigen display have minimal influence on the kinetics of the CD4+ T-cell response to *Listeria monocytogenes* infection. J. Immunol. **173:**5679–5687.
9. **Fang, R., N. Ismail, L. Soong, V. L. Popov, T. Whitworth, D. H. Bouyer, and D. H. Walker.** 2007. Differential interaction of dendritic cells with *Rickettsia conorii*: impact on host susceptibility to murine spotted fever rickettsiosis. Infect. Immun. **75:**3112–3123.
10. **Frischknecht, F.** 2007. The skin as interface in the transmission of arthropod-borne pathogens. Cell Microbiol. **9:**1630–1640.
11. **Heath, W. R., G. T. Belz, G. M. Behrens, C. M. Smith, S. P. Forehan, I. A. Parish, G. M. Davey, N. S. Wilson, F. R. Carbone, and J. A. Villadangos.** 2004. Cross-presentation, dendritic cell subsets, and the generation of immunity to cellular antigens. Immunol. Rev. **199:**9–26.
12. **Hopkins, S. A., F. Niedergang, I. E. Corthesy-Theulaz, and J. P. Kraehenbuhl.** 2000. A recombinant *Salmonella typhimurium* vaccine strain is taken up and survives within murine Peyer's patch dendritic cells. Cell Microbiol. **2:**59–68.
13. **Itano, A. A., and M. K. Jenkins.** 2003. Antigen presentation to naive CD4 T cells in the lymph node. Nat. Immunol. **4:**733–739.
14. **Itano, A. A., S. J. McSorley, R. L. Reinhardt, B. D. Ehst, E. Ingulli, A. Y. Rudensky, and M. K. Jenkins.** 2003. Distinct dendritic cell populations sequentially present antigen to CD4 T cells and stimulate different aspects of cell-mediated immunity. Immunity **19:**47–57.
15. **Jelley-Gibbs, D. M., D. M. Brown, J. P. Dibble, L. Haynes, S. M. Eaton, and S. L. Swain.** 2005. Unexpected prolonged presentation of influenza antigens promotes CD4 T cell memory generation. J. Exp. Med. **202:**697–706.
16. **Jung, Y. J., L. Ryan, R. Lacourse, and R. J. North.** 2005. Properties and protective value of the secondary versus primary T helper type 1 response to airborne *Mycobacterium tuberculosis* infection in mice. J. Exp. Med. **201:**1915–1924.
17. **Lawrence, C. W., and T. J. Braciale.** 2004. Activation, differentiation, and migration of naive virus-specific CD8+ T cells during pulmonary influenza virus infection. J. Immunol. **173:**1209–1218.
18. **Li, J. S., F. Chu, A. Reilly, and G. M. Winslow.** 2002. Antibodies highly effective in SCID mice during infection by the intracellular bacterium *Ehrlichia chaffeensis* are of picomolar affinity and exhibit preferential epitope and isotype utilization. J. Immunol. **169:**1419–1425.
19. **Li, J. S., E. Yager, M. Reilly, C. Freeman, G. R. Reddy, F. K. Chu, and G. Winslow.** 2001. Outer membrane protein specific monoclonal antibodies protect SCID mice from fatal infection by the obligate intracellular bacterial pathogen *Ehrlichia chaffeensis*. J. Immunol. **166:**1855–1862.
20. **Lopes-Carvalho, T., J. Foote, and J. F. Kearney.** 2005. Marginal zone B cells in lymphocyte activation and regulation. Curr. Opin. Immunol. **17:**244–250.
21. **Maender, J. L., and S. K. Tyring.** 2004. Treatment and prevention of rickettsial and ehrlichial infections. Dermatol. Ther. **17:**499–504.
22. **McMahon, C. W., A. J. Zajac, A. M. Jamieson, L. Corral, G. E. Hammer, R. Ahmed, and D. H. Raulet.** 2002. Viral and bacterial infections induce expression of multiple NK cell receptors in responding CD8$^+$ T cells. J. Immunol. **169:**1444–1452.

23. **Mix, D., and G. M. Winslow.** 1996. Proteolytic processing activates a viral superantigen. J. Exp. Med. **184:**1549–1554.
24. **Miyahira, Y., K. Murata, D. Rodriguez, J. R. Rodriguez, M. Esteban, M. M. Rodrigues, and F. Zavala.** 1995. Quantification of antigen specific CD8+ T cells using an ELISPOT assay. J. Immunol. Methods **181:**45–54.
25. **Monack, D. M., A. Mueller, and S. Falkow.** 2004. Persistent bacterial infections: the interface of the pathogen and the host immune system. Nat. Rev. Microbiol. **2:**747–765.
26. **Nandi, B., K. Hogle, N. Vitko, and G. Winslow.** 2007. CD4 T cell epitopes associated with protective immunity induced following vaccination of mice with an ehrlichia variable outer membrane protein. Infect. Immun. **75:**5453–5459.
27. **Neuenhahn, M., K. M. Kerksiek, M. Nauerth, M. H. Suhre, M. Schiemann, F. E. Gebhardt, C. Stemberger, K. Panthel, S. Schroder, T. Chakraborty, S. Jung, H. Hochrein, H. Russmann, T. Brocker, and D. H. Busch.** 2006. $CD8\alpha^+$ dendritic cells are required for efficient entry of Listeria monocytogenes into the spleen. Immunity **25:**619–630.
28. **Norbury, C. C., D. Malide, J. S. Gibbs, J. R. Bennink, and J. W. Yewdell.** 2002. Visualizing priming of virus-specific CD8+ T cells by infected dendritic cells in vivo. Nat. Immunol. **3:**265–271.
29. **North, R. J., and Y. J. Jung.** 2004. Immunity to tuberculosis. Annu. Rev. Immunol. **22:**599–623.
30. **Noss, E. H., C. V. Harding, and W. H. Boom.** 2000. *Mycobacterium tuberculosis* inhibits MHC class II antigen processing in murine bone marrow macrophages. Cell Immunol. **201:**63–74.
31. **Olano, J. P., G. Wen, H. M. Feng, J. W. McBride, and D. H. Walker.** 2004. Histologic, serologic, and molecular analysis of persistent ehrlichiosis in a murine model. Am. J. Pathol. **165:**997–1006.
32. **Paddock, C. D., and J. E. Childs.** 2003. *Ehrlichia chaffeensis*: a prototypical emerging pathogen. Clin. Microbiol. Rev. **16:**37–64.
33. **Pamer, E. G.** 2004. Immune responses to *Listeria monocytogenes*. Nat. Rev. Immunol. **4:**812–823.
34. **Quah, B. J., H. S. Warren, and C. R. Parish.** 2007. Monitoring lymphocyte proliferation in vitro and in vivo with the intracellular fluorescent dye carboxyfluorescein diacetate succinimidyl ester. Nat. Protoc. **2:**2049–2056.
35. **Reis e Sousa, C.** 2006. Dendritic cells in a mature age. Nat. Rev. Immunol. **6:**476–483.
36. **Rikihisa, Y.** 2006. Ehrlichia subversion of host innate responses. Curr. Opin. Microbiol. **9:**95–101.
37. **Shibata, S., M. Kawahara, Y. Rikihisa, H. Fujita, Y. Watanabe, C. Suto, and T. Ito.** 2000. New Ehrlichia species closely related to *Ehrlichia chaffeensis* isolated from *Ixodes ovatus* ticks in Japan. J. Clin. Microbiol. **38:**1331–1338.
38. **Shortman, K., and Y. J. Liu.** 2002. Mouse and human dendritic cell subtypes. Nat. Rev. Immunol. **2:**151–161.
39. **Sotomayor, E. A., V. L. Popov, H. M. Feng, D. H. Walker, and J. P. Olano.** 2001. Animal model of fatal human monocytotropic ehrlichiosis. Am. J. Pathol. **158:**757–769.
40. **Stevenson, H. L., J. M. Jordan, Z. Peerwani, H. Q. Wang, D. H. Walker, and N. Ismail.** 2006. An intradermal environment promotes a protective type-1 response against lethal systemic monocytotropic ehrlichial infection. Infect. Immun. **74:**4856–4864.
41. **Tailleux, L., O. Schwartz, J.-L. Herrmann, E. Pivert, M. Jackson, A. Amara, L. Legres, D. Dreher, L. P. Nicod, J. C. Gluckman, P. H. Lagrange, B. Gicquel, and O. Neyrolles.** 2002. DC-SIGN is the major *Mycobacterium tuberculosis* receptor on human dendritic cells. J. Exp. Med. **197:**121–127.
42. **Thimme, R., V. Appay, M. Koschella, E. Panther, E. Roth, A. D. Hislop, A. B. Rickinson, S. L. Rowland-Jones, H. E. Blum, and H. Pircher.** 2005. Increased expression of the NK cell receptor KLRG1 by virus-specific CD8 T cells during persistent antigen stimulation. J. Virol. **79:**12112–12116.
43. **Ting, L. M., A. C. Kim, A. Cattamanchi, and J. D. Ernst.** 1999. *Mycobacterium tuberculosis* inhibits IFN-gamma transcriptional responses without inhibiting activation of STAT1. J. Immunol. **163:**3898–3906.
44. **Turner, D. L., L. S. Cauley, K. M. Khanna, and L. Lefrancois.** 2007. Persistent antigen presentation after acute vesicular stomatitis virus infection. J. Virol. **81:**2039–2046.
45. **van der Most, R. G., K. Murali-Krishna, and R. Ahmed.** 2003. Prolonged presence of effector-memory CD8 T cells in the central nervous system after dengue virus encephalitis. Int. Immunol. **15:**119–125.
46. **Voehringer, D., C. Blaser, P. Brawand, D. H. Raulet, T. Hanke, and H. Pircher.** 2001. Viral infections induce abundant numbers of senescent CD8 T cells. J. Immunol. **167:**4838–4843.
47. **Wen, B., Y. Rikihisa, J. Mott, P. A. Fuerst, M. Kawahara, and C. Suto.** 1995. *Ehrlichia muris* sp. nov., identified on the basis of 16S rRNA base sequences and serological, morphological, and biological characteristics. Int. J. Syst. Bacteriol. **45:**250–254.
48. **Winslow, G. M., A. D. Roberts, M. A. Blackman, and D. L. Woodland.** 2003. Persistence and turnover of antigen-specific CD4 T cells during chronic tuberculosis infection in the mouse. J. Immunol. **170:**2046–2052.
49. **Wolf, A. J., B. Linas, G. J. Trevejo-Nunez, E. Kincaid, T. Tamura, K. Takatsu, and J. D. Ernst.** 2007. *Mycobacterium tuberculosis* infects dendritic cells with high frequency and impairs their function in vivo. J. Immunol. **179:**2509–2519.
50. **Young, D., T. Hussell, and G. Dougan.** 2002. Chronic bacterial infections: living with unwanted guests. Nat. Immunol. **3:**1026–1032.
51. **Zajac, A. J., J. N. Blattman, K. Murali-Krishna, D. J. Sourdive, M. Suresh, J. D. Altman, and R. Ahmed.** 1998. Viral immune evasion due to persistence of activated T cells without effector function. J. Exp. Med. **188:**2205–2213.
52. **Zammit, D. J., D. L. Turner, K. D. Klonowski, L. Lefrancois, and L. S. Cauley.** 2006. Residual antigen presentation after influenza virus infection affects CD8 T cell activation and migration. Immunity **24:**439–449.
53. **Zhang, J. Z., M. Sinha, B. A. Luxon, and X. J. Yu.** 2004. Survival strategy of obligately intracellular *Ehrlichia chaffeensis*: novel modulation of immune response and host cell cycles. Infect. Immun. **72:**498–507.
54. **Zhou, Y., D. Ray, Y. Zhao, H. Dong, S. Ren, Z. Li, Y. Guo, K. A. Bernard, P. Y. Shi, and H. Li.** 2007. Structure and function of flavivirus NS5 methyltransferase. J. Virol. **81:**3891–3903.

Editor: R. P. Morrison